



HAL
open science

Computing Execution Times with eXecution Decision Diagrams in the Presence of Out-Of-Order Resources

Zhenyu Bai, Hugues Cassé, Thomas Carle, Christine Rochange

► **To cite this version:**

Zhenyu Bai, Hugues Cassé, Thomas Carle, Christine Rochange. Computing Execution Times with eXecution Decision Diagrams in the Presence of Out-Of-Order Resources. IEEE Transactions on Computer-Aided Design of Integrated Circuits and Systems, 2023, 42 (11), pp.3665-3678. 10.1109/TCAD.2023.3258752 . hal-04069420

HAL Id: hal-04069420

<https://hal.science/hal-04069420v1>

Submitted on 14 Apr 2023

HAL is a multi-disciplinary open access archive for the deposit and dissemination of scientific research documents, whether they are published or not. The documents may come from teaching and research institutions in France or abroad, or from public or private research centers.

L'archive ouverte pluridisciplinaire **HAL**, est destinée au dépôt et à la diffusion de documents scientifiques de niveau recherche, publiés ou non, émanant des établissements d'enseignement et de recherche français ou étrangers, des laboratoires publics ou privés.



Distributed under a Creative Commons Attribution - NonCommercial 4.0 International License

Computing Execution Times with eXecution Decision Diagrams in the Presence of Out-Of-Order Resources

Zhenyu Bai
Hugues Cassé
Thomas Carle
Christine Rochange

IRIT, Université de Toulouse, CNRS, Toulouse INP, UT3, 118 route de Narbonne 31062 Toulouse, France
Email: *firstname.surname@irit.fr*

Abstract—We propose a precise and efficient pipeline analysis to tackle the problem of out-of-order resources in modern embedded microprocessors for the computation of the Worst-Case Execution Time (WCET). Such resources are prone to timing anomalies [1]. To remain sound, the timing analysis must either rely on huge timing over-estimations or consider all possible pipeline states which usually leads to a combinatorial blowup. To cope with this situation, we build an efficient computational model by leveraging the algebraic properties of the eXecution Decision Diagram [2] which is able to track precisely all pipeline states all along the execution paths of the analysed program while keeping the analysis time within acceptable range. We show how to apply this analysis at the Control Flow Graph (CFG) level, and how to account for a typical out-of-order resource: the shared memory bus between the instruction and data caches. We observe a gain in precision of the WCET ranging from 20% to 80% compared to the state-of-the-art pipeline analysis of the OTAWA WCET toolset. The analysis time shows that our approach scales to realistic benchmarks, making it appropriate for industrial applications.

Index Terms—real-time, WCET, static analysis, pipeline

I. INTRODUCTION

The correctness of hard real-time systems depends not only on their functional behavior but also on their temporal behavior. The latter is guaranteed by the scheduling analysis of the tasks composing the system, which relies on the estimation of their Worst-Case Execution Time (WCET).

With modern processors, the execution time of a code snippet is difficult to determine. For instance, on a processor equipped with cache memories, the latency of memory accesses is variable: it depends on whether the access results in a *Cache Miss* or a *Cache Hit*. The presence, in modern micro-architectures, of pipelined and superscalar execution and other mechanisms to favor instruction-level parallelism and achieve high performance generates a large variability of execution times and makes the WCET analysis suffer from *timing anomalies* [3]–[6]. Briefly, timing anomalies imply that the WCET analysis cannot assume that a local worst case will lead to the global worst case. Illustrated on the case of cache accesses, this means that a cache miss (longer access) cannot

be assumed to lead to the global worst case, and whether or not it contributes to the global WCET is not determined [1], [7]. Unless the target processor is proven to be free of timing anomalies, a safe and precise WCET analysis has to capture them by precisely tracking the execution states of the micro-architecture.

The WCET computation is generally broken down into three parts [8]. First, *global analyses*, independent of the pipeline's structure, are performed: they typically encompass cache and branch-prediction analyses, which determine the behavior of these mechanisms at instruction level. Second, the *pipeline analysis* uses the information provided by *global analyses* to determine how instructions are executed through the pipeline, and to compute the (worst-case) execution times of basic blocks (BB). Finally, an ILP system is built to maximize the execution time considering the individual WCETs of basic blocks computed in the previous step, with constraints expressing the structure of the CFG and flow facts, such as loop bounds. The solution of the ILP system is the WCET of the whole program. This method is called *Implicit Path Enumeration Technique* (IPET) [9].

The most important bottleneck in the classical structure of WCET analysis is the lack of efficient abstraction of pipeline. Existing approaches either tend to be not scalable or imprecise. However, our previous approach [2] shows that the eXecution Decision Diagram (XDD) is a good data structure to record times within the pipeline analysis that improves its performance. An XDD can be deemed as a lossless compression of the relationship between the execution time and the combination of timing variations. By implanting XDD into the Execution Graph (XG) pipeline model, we achieved exact and efficient pipeline analysis on basic blocks through in-order pipelines. In [2], the pipeline analysis is designed to consider BBs of a program independently by calculating their worst-case execution context. However, with out-of-order accesses to resources such as shared buses, the conservative use of a worst-case context does not hold anymore. We need to precisely track the possible execution contexts in order to evaluate how the

concurrent accesses to the bus are interleaved. The pipeline analysis has to analyze the micro-architecture states on the whole program, that is, at Control-Flow Graph (CFG) level.

a) Contributions: This paper presents (a) how we adapt the original graph based pipeline model proposed in [2] into a data-flow analysis applied at CFG level that computes exactly all the possible temporal pipeline states; (b) how we construct an efficient computational model of our analysis by leveraging the algebraic properties of XDD, which turns the state transition into matrix multiplication on a semi-ring; (c) how we exploit the precise pipeline states produced by this computational model to support a typical out-of-order resource: the memory bus that is shared by the instruction and data caches to access the main memory; and (d) the evaluation of our model on realistic applications (TACLe’s benchmarks [10]) that shows its scalability. Several parameters are measured during the experiment to give some explanation of its good performance. The precision gain of our approach is compared with the state-of-the-art pipeline analysis of *OTAWA* [11] and shows improvement of the final WCET ranging from 20% to 80%.

b) Outline: First, the related works are discussed in Section II. Section III provides background information on the XG model and the XDD structure. In Section IV, we extend the original model of XG with XDD to a resource-based model which is able to express the state of the pipeline with a vector. Later in this section, we show how to leverage the algebraic properties of XDD in order to improve the performance of the analysis by pre-computing the calculus as matrices. In Section V, we show how to build the complete analysis at CFG level. Section VI extends our model to support the shared memory bus. Experiments reported in Section VII demonstrate the efficiency and the precision of our analysis on realistic benchmarks. Several metrics are considered and discussed, and we conclude in Section VIII.

II. RELATED WORK

The most complex part of the classical structure of WCET analysis (global analyses + pipeline analysis + IPET) is the pipeline analysis because of the presence of timing anomalies and the complexity of modern micro-architectures. We may classify the state-of-the-art pipeline analyses into two classes: those at CFG level and those at BB level.

The aiT analyzer is one of the most successful WCET analysis tools and it performs pipeline analysis at CFG level [12], [13]. Concretely, it builds an abstract model of the pipeline: this model describes the transition of pipeline states at the granularity of processor cycles. Its pipeline analysis, based on the abstract interpretation framework [14], computes an overset of the possible pipeline states over the CFG of the program. To the best of our knowledge, it uses power set domain to keep the set of possible pipeline states. Therefore, this model suffers from combinatorial complexity caused by the presence of timing anomalies as it has to keep all possible states. Several approaches were proposed to reduce the complexity: (a) although the literature provides very few details

about that, close states seem to be joined to form abstract states at the cost of a loss of precision, (b) in [15], the authors show how to use a Binary Decision Diagram to compress the state machine representation of their analysis system, and (c) in [16] Reineke et al. define a sufficient condition to drop *not-worst* cases in order to reduce the number of states. This work has been extended later in [17], [18], providing a theoretical basis to design strictly-in-order pipeline where timing anomalies are proven to not occur [7], [19], thus allowing to more easily drop non-worst case states.

Another approach to pipeline analysis is to compute locally the WCET per BB. The *Execution Graph* proposed by Li et al. [20] (chronos analyzer) is a very representative example. Instead of computing the pipeline state over the CFG, they make assumptions about the worst execution context of each BB. To avoid using powerset domain to keep the pipeline states, they use interval domain to keep the minimal and maximal execution times of instructions. The contention between instructions is considered by checking the intersection of time intervals. If a contention occurs, the interval is extended accordingly. The XG solving algorithm repeats the computation until a fix point is reached. However, in the presence of lots of events, the interval representation tends to trigger a chain reaction: the imprecision due to the interval representation creates contentions that are actually impossible, which extends the interval and involves more impossible contentions – hence introducing considerable over-estimation. Moreover, with respect to the micro-architecture, making precise assumptions on the worst execution context is not always simple. Another XG-based approach is proposed by Rochange et al. in [21] that computes the execution time of BBs for each combination of events, which makes the algorithm tending towards combinatorial complexity. In addition, the contention analysis requires examining all cases, leading to an exponential complexity.

Another different direction of static WCET analysis uses model checking approaches. The principle of these approaches is to express the analyzed program and the complete micro-architecture (including cache, pipeline and all timing related components) by a timed automaton without abstraction. The WCET is computed by exploring all possible states of the automaton. Since all states are reached, it is compatible with timing anomalies by nature. These approaches usually provide exact WCETs and are able to give the longest path, which may help the developers to further optimize the WCET. On the other hand, they generally have scalability issues when the micro-architecture becomes complex (this results in a larger pipeline state domain) or when the program under analysis becomes complex (this results in an intractable amount of execution traces to explore). One of the most well known tools in this category is UPPAAL [22]. To the best of our knowledge, the best experiment using UPPAAL, reported in [23], is not able to analyze all the benchmarks of the Mälardalen suite, but only the simplest ones. Some hypotheses are also made to turn some programs into single-path programs, which greatly reduces the complexity of the problem.

In [24], the authors compute the WCET of BBs with *reservation tables* that simulate the reservation of resources in the pipeline at each cycle. The worst reservation hence gives the worst execution time. In [25], the worst behavior of the pipeline, caches and branch predictors are obtained by simulations at BB-level. In [26], the worst timing contributions of different components (cache, pipeline and others) are computed separately and then safely composed using rules defined in the paper. In [27], the authors bound the distance of temporal effects between instructions, so as to compute the WCET per instruction with a safe over-estimation.

Our analysis: The pipeline model proposed in this paper is inspired from a key idea of the XG approach: it uses dependencies to describe the temporal behavior of the pipeline, which allows the analysis to work at pipeline stage level (unlike aiT that works at the granularity of processor cycles). Our strategy improves the efficiency of the analysis because one dependency often spans over several processor cycles, which leads to a reduced number of applied transitions and a more compact dependency representation.

Compared to the original XG approach, this new model considers the effect of instructions of other BBs on the timing of the analyzed BB (instead of considering each BB in isolation), and it uses XDDs (instead of the interval domain in the original XG, or the powerset domain in the case of aiT) to efficiently represent all possible pipeline states without loss of precision. Theoretically, this approach is thus more precise than the original XG approach, and more efficient than the approach used by aiT when tracking explicitly all possible pipeline states.

III. BACKGROUND

As a program under analysis usually has several execution paths and possibly loops, it is impossible to track all the possible execution traces. The static WCET analysis approach we use in this paper models the whole program as a CFG, then computes the WCET of each BB and determines the WCET using the IPET method. Thus, the pipeline analysis aims at determining the execution time of each BB, for example, using *Execution Graphs*.

A. Execution Graphs

An eXecution Graph (XG) [20], [21] models the temporal behavior of an instruction sequence (such as a BB) executed in the pipeline. The key idea of the XG is to model the temporal behavior by considering the dependencies arising between instructions during their execution in the pipeline stages. For example, an instruction has to leave a pipeline stage before starting its execution in the next stage, an instruction has to read a register after a prior instruction has written this register, etc. This results in a dependency graph: a vertex represents the progress of an instruction in a pipeline stage; the edges represent the precedence relationships between these vertices. Formally, let \mathcal{I} be the set of machine instructions, and let G_{XG} be a *Directed Acyclic Graph* (DAG) $G_{XG} = \langle V_{XG}, E_{XG} \rangle$ built for an instruction sequence \mathcal{I}^* such that

- V_{XG} is the set of vertices defined by $V_{XG} = \{[I_i/s] \mid I_i \in \mathcal{I}^* \wedge s \in \mathcal{P}\}$, with \mathcal{P} the set of pipeline stages.
- $E_{XG} \subset V_{XG} \times V_{XG}$, the set of edges, is built according to the dependencies in the considered pipeline.

In addition, an XG is decorated with temporal information:

- $\lambda_v \in \mathbb{N}$ is the latency of vertex v , that is the time spent in this vertex.
- $\delta_{v \rightarrow w} \in \{0, 1\}$ represents the kind of dependency expressed by edge $v \rightarrow w \in E_{XG}$. If $\delta_{v \rightarrow w} = 1$ (solid), w starts after the end of v ; if $\delta_{v \rightarrow w} = 0$ (dotted), w can start at the same time as or after the start of v .

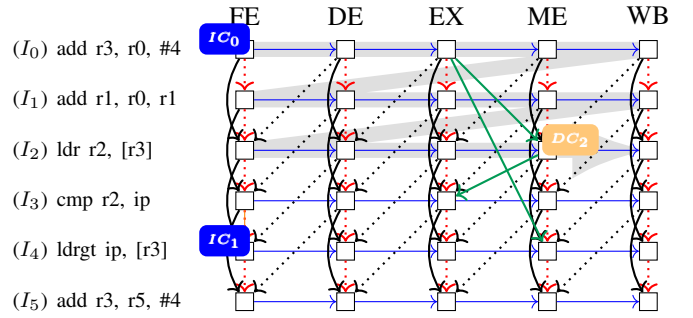


Fig. 1: XG model of an instruction sequence.

Examples in this paper consider a 5-stage (FE – fetch, DE – decode, EX – execute, ME – memory, WB – write-back) in-order 2-way superscalar pipeline but the presented algorithms are not limited to this configuration. Figure 1 shows the XG for this pipeline and for the sequence of instructions listed on the left. The vertices correspond to the use of a pipeline stage (column headers) by an instruction (row headers). The edges reflect the following dependencies:

- The horizontal solid edges model the *Pipeline Order*: an instruction goes through pipeline stages in a given order.
- The vertical dotted edges model the parallel execution of instructions in the superscalar stages (*Program Order*).
- The vertical solid bent edges model the width of the stages – 2 instructions per cycle (*Capacity Order*).
- The slanted dotted edges model the capacity of FIFO queues (2 instructions) between stages (*Queue Capacity*).
- The slanted solid edges model the *Data Dependencies* between instructions, when an instruction reads a register written by a prior instruction.

The set of dependency edges shown above is typical for in-order pipelines. Depending on a particular pipeline design, rules to build the edges may be added or removed to account for specific features.

Using an XG, the start time of an instruction in a stage ρ_w is computed as the earliest time at which all incoming dependencies are satisfied and the end time ρ_w^* as ρ_w increased by the time passed by the instruction in the stage:

$$\begin{aligned} \rho_w &= \max_{v \rightarrow w \in E_{XG}} \rho_v + \delta_{v \rightarrow w} \times \lambda_v \\ \rho_w^* &= \rho_w + \lambda_w \end{aligned} \quad (1)$$

The execution time of the instruction sequence is obtained by calculating the start time of each vertex following a topological order in the XG. Since the pipeline is in-order (all resources are allocated in the program order), the timing of an instruction only depends on prior instructions, meaning that, at least, one topological order exists. For in-order processors, this order is implied by the combination of the *Pipeline Order* (horizontal edges) and of the *Capacity Order* (vertical edges). It is highlighted in the example XG of Figure 1 by the light gray arrow in the background.

The computation of an XG is fast and efficient. However, as soon as the pipeline produces variable latencies (e.g. to reflect a possible cache hit or miss), precision is achieved at the cost of computing the XG for each combination of these latencies. This may engender a computation complexity explosion. The data structure presented in the next section alleviates this issue.

B. Execution Decision Diagrams

The eXecution Decision Diagram (XDD) is inspired from the Binary Decision Diagram (BDD) [28], [29] and its Multi-Terminal BDD (MTBDD) variant [30]. An XDD is a DAG that is recursively defined as:

Definition III.1.

$$\text{XDD} = \text{LEAF}(k) \mid \text{NODE}(e, \bar{f}, f) \quad (2)$$

The Boolean variables $e \in \mathcal{E}$ in nodes are called *events*: they model the uncertainty in the analysis regarding the micro-architecture state and its impact on the time, e.g. whether a particular cache access results in a hit or in a miss. The subtrees $f, \bar{f} \in \text{XDD}$ represent, respectively, the situations where the event e happens or not. The leaves of an XDD store the execution times $k \in \mathbb{Z}^\# = \mathbb{Z} \cup \{+\infty, -\infty\}$.

As in ordered BDDs [29], XDDs deploy hash consing techniques to guarantee the unicity of the sub-tree instances and speed up the calculation: identical sub-trees share the same instance in memory. This compression allows the XDDs to represent efficiently the relationships between combinations of events (called *configurations*) and the corresponding execution times. A configuration $\gamma \in \Gamma$ is the combination of activation or inactivation of events ($\Gamma = \wp(\mathcal{E})$) and corresponds to a path from the root node to a leaf in the XDD DAG.

When events are taken into account, the actual time for each vertex is represented by a map between event configurations and the corresponding times (i.e. in the domain $\Gamma \rightarrow \mathbb{Z}^\#$) the size of which is combinatorial with respect to the number of events (which determines the cost in terms of computation time). XDDs efficiently solve this problem by factorizing identical sub-trees. In [2], it has been shown that the subtree factorization frequently occurs in realistic benchmarks which largely speeds up the analysis. Yet, an isomorphism between XDD and $\Gamma \rightarrow \mathbb{Z}^\#$ exists: $\text{XDD} \xrightleftharpoons[\beta]{\alpha} (\Gamma \rightarrow \mathbb{Z}^\#)$. This means that XDD can be deemed as a lossless compression of the map $(\Gamma \rightarrow \mathbb{Z}^\#)$. In the remainder of the paper, we note $f[\gamma]$ the time corresponding to configuration γ in f (for $f \in \text{XDD}$

or $f \in \Gamma \rightarrow \mathbb{Z}^\#$ since both are equivalent from a functional point of view).

In [2], it was shown that any binary operation \odot on $\mathbb{Z}^\#$ used in $(\Gamma \rightarrow \mathbb{Z}^\#)$ can be transferred in the XDD domain in an equivalent operation \boxtimes such that performing the operation in the XDD domain is lossless:

$$\begin{aligned} \forall s_1, s_2 \in (\Gamma \rightarrow \mathbb{Z}^\#)^2, \forall \gamma \in \Gamma, \\ s_1[\gamma] \odot s_2[\gamma] = (\alpha(s_1) \boxtimes \alpha(s_2))[\gamma] \end{aligned} \quad (3)$$

with α the morphism from $(\Gamma \rightarrow \mathbb{Z}^\#)$ to XDD.

The operations used in XG are *max* and $+$ (Eq. (1)). These two operations are transferred into the domain of XDD, respectively \oplus and \otimes^1 , such that the time corresponding to each configuration in the resulting XDD is exactly the time computed for each configuration without XDD:

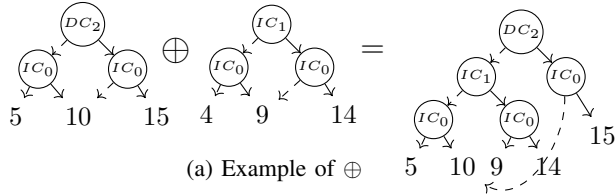
$$\begin{aligned} \forall s_1, s_2 \in (\Gamma \rightarrow \mathbb{Z}^\#)^2, \forall \gamma \in \Gamma, \\ s_1[\gamma] + s_2[\gamma] = (\alpha(s_1) \otimes \alpha(s_2))[\gamma] \\ \max(s_1[\gamma], s_2[\gamma]) = (\alpha(s_1) \oplus \alpha(s_2))[\gamma] \end{aligned} \quad (4)$$

The implementation of this operation is detailed in [2]. Shortly, \boxtimes combines XDD operands along sub-trees and applies \odot when leaves need to be combined.

Now, one can implant XDDs into the XG computation (Eq. (1)) by replacing *max* by \oplus and $+$ by \otimes . Each ρ in equation (1) now becomes a XDD recording all execution times with respect to the configurations of events. By doing that, we now compute all execution times in a single traversal of the XG. Let us consider some concrete examples in the computation of the XG showed in Figure 1 with XDDs. Three events are considered and highlighted in the figure: IC_0, IC_1 and DC_2 . The IC events are instruction cache events, meaning that the associate instruction fetch may result in instruction cache miss, leading to an increased latency; DC_2 is a data cache event. The extra latency of both types of events is 5 cycles. Figure 2a shows the use of \oplus when computing the start date of $[I_4/EX]$ where the first operand is the start date of $[I_3/EX]$ and the second operand is the end date of $[I_4/DE]$. Figure 2b shows the explicit representation of the resulting XDD in Figure 2a. Figure 2c shows the use of \otimes when computing the end time ρ^* of $[I_2/ME]$: the first operand is the start time and the second operand is the latency of $[I_2/ME]$.

The isomorphism guarantees that using an XDD to perform the XG analysis is *precise* by following the dependency resolution rule (Eq. (1)) and the proposed topological order. However, the graph can only be built for sequentially executed instructions which raises difficulties for the pipeline analysis at CFG level. Hence, the next section proposes a pipeline analysis in the paradigm of state machine which can be easily adapted for the analysis at CFG level and allows to leverage algebraic property of XDD to speed up the computation.

¹It must be emphasized that the name of the transferred operators is not related to the original operator: \oplus does not correspond to $+$ but *max*, and it is \otimes that corresponds to $+$, this is due to the algebra property of XDD semi-ring that we will mention later in section IV-C.

(a) Example of \oplus

Configuration	time
IC_0, IC_1, DC_2	15
$IC_0, \overline{IC}_1, DC_2$	15
$\overline{IC}_0, IC_1, DC_2$	10
$\overline{IC}_0, \overline{IC}_1, DC_2$	10
$IC_0, IC_1, \overline{DC}_2$	14
$\overline{IC}_0, IC_1, \overline{DC}_2$	9
$IC_0, \overline{IC}_1, \overline{DC}_2$	10
$\overline{IC}_0, \overline{IC}_1, \overline{DC}_2$	5

(b) Explicit representation

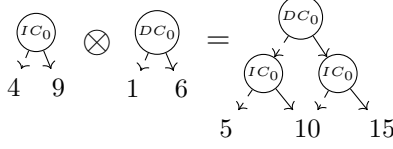
(c) Example of \otimes

Fig. 2: Example of XDDs

IV. RESOURCE BASED MODEL

The usual approach, that consists in building and solving an XG for each BB on its own, is no more sustainable when out-of-order bus accesses have to be supported. The bus access interactions can indeed span over BB bounds.

This section proposes to solve this issue by turning the original XG model into a state machine model where the pipeline analysis is performed by applying transitions on pipeline states. Moreover, by leveraging the algebraic property of XDDs, we improve the computational model by implementing transitions as products of matrices. The matrices can be pre-computed before the pipeline analysis.

A. Temporal State

The dependencies $d \in \mathcal{D}$ in the XG model the use of *resources*, such as pipeline stages, queues etc. For instance, in our 5-stage in-order pipeline, determining the start time of an instruction $I_i \in \mathcal{I}^*$ in stage DE requires:

- the start time of the previous instruction in stage DE : $\rho_{[I_{i-1}/DE]}$ – the Program Order dependency due to the use of DE stage in program order,
- the end time of the second last instruction in stage DE : $\rho_{[I_{i-2}/DE]}^*$ – the Capacity Order dependency due to the use of DE stage with limited capacity,
- the end time of I_i in stage FE : $\rho_{[I_i/FE]}^*$ – the Pipeline Order dependency due to the use of the pipeline,
- the start time of the second last instruction in stage EX : $\rho_{[I_{i-2}/EX]}$ – the Queue Capacity dependency due to the use of the queue between DE and EX with limited capacity.

where I_{i-n} represents the n^{th} previous instruction. $\rho_{[I_i/s]}$ and $\rho_{[I_i/s]}^*$ respectively stand for the start and the end time of vertex $[I_i/s]$. The actual start time of I_i in DE is the earliest date at which all dependencies are satisfied:

$$\begin{aligned} \rho_{[I_i/DE]} &= \rho_{[I_{i-1}/DE]} \oplus \rho_{[I_{i-2}/DE]}^* \\ &\oplus \rho_{[I_i/FE]}^* \oplus \rho_{[I_{i-2}/EX]} \\ \rho_{[I_{i-2}/DE]}^* &= \rho_{[I_{i-2}/DE]} \otimes \lambda_{[I_{i-2}/DE]} \\ \rho_{[I_i/FE]}^* &= \rho_{[I_i/FE]} \otimes \lambda_{[I_i/FE]} \end{aligned}$$

This corresponds to the computation of Eq. (1) extended to the XDD domain: we use \oplus instead of max and \otimes instead of $+$. As in the integer case, each computation requires the results of the computations of previous instructions (e.g. $\rho_{[I_i/DE]}$ requires $\rho_{[I_{i-1}/DE]}$ and $\rho_{[I_{i-2}/DE]}^*$), which correspond to the release time of the concerned resources.

Table I shows the information required to compute the start time of any instruction I_i in stage DE : it forms a *vector* of 6 elements, each element being an XDD. The vector depends on the structure of the pipeline, but an important point is that any architecture that can be described in the XG model can also be expressed as a vector of XDDs.

Such a vector can be similarly built for each instruction and each pipeline stage. Table II shows the complete dependency information to be maintained for each stage of our example pipeline. The symbol $-\infty$ denotes the absence of dependency². I_{fetch} , I_{load} , I_{store} and I_{R_i} are, respectively, the last instructions that have fetched an instruction block from memory, performed a load, performed a store and wrote to register R_i (in stage s_{R_i}).

Let \mathcal{D} be the set of dependencies listed in Table II. The *temporal state* of the pipeline can be represented by a vector in the domain $\mathcal{S} = \text{XDD}^{|\mathcal{D}|}$. For a given stage s , a temporal state $\vec{S} \in \mathcal{S}$, and the set of dependencies $\mathcal{D}_{[I_i/s]} \subset \mathcal{D}$ applicable to XG vertex $[I_i/s]$, the start and end times of this vertex can now be rewritten as:

$$\rho_{[I_i/s]} = \bigoplus_{d \in \mathcal{D}_{[I_i/s]}} \vec{S}[i_d] \quad (5)$$

$$\rho_{[I_i/s]}^* = \rho_{[I_i/s]} \otimes \lambda_{[I_i/s]} \quad (6)$$

where i_d denotes the index of dependency d within vector \vec{S} .

B. Pipeline Analysis with Temporal States

We now present how temporal states are updated during the analysis to account for the execution of instructions in the pipeline. To simplify the computation, we add an element ϱ at index i_ϱ to the state vector. It records the *current time* all along the analysis: we refer to ϱ as the *time pointer*.

Definition IV.1. Following the principle of XG analysis, the behavior of an instruction in a pipeline stage can be broken down into four steps.

- Step 1. The instruction cannot be executed in the stage before all its dependencies are satisfied (Eq. (5)). This is modelled as follows. First, the time pointer is reset to $\emptyset = LEAF(-\infty)$ (Step 1.1). Then, each dependency time is accumulated with \oplus into the time pointer (Step 1.2). At the end of Step 1, the time pointer records the maximum

² $-\infty$ is convenient as it is neutral for the max operation.

TABLE I: Information needed to determine the start time of any I_i in stage DE

Program Order	Capacity Order		Pipeline Order	Queue Capacity	
$\rho_{[I_{i-1}/DE]}$	$\rho_{[I_{i-2}/DE]}^*$	$\rho_{[I_{i-1}/DE]}^*$	$\rho_{[I_i/FE]}^*$	$\rho_{[I_{i-2}/EX]}$	$\rho_{[I_{i-1}/EX]}$

 TABLE II: The *temporal state*

	Prog. Order	Capacity Order		Pipeline Order	Queue Capacity	
FE	$\rho_{[I_{i-1}/FE]}$	$\rho_{[I_{i-1}/FE]}^*$	$\rho_{[I_{i-2}/FE]}^*$	$-\infty$	$\rho_{[I_{i-1}/DE]}$	$\rho_{[I_{i-2}/DE]}$
DE	$\rho_{[I_{i-1}/DE]}$	$\rho_{[I_{i-1}/DE]}^*$	$\rho_{[I_{i-2}/DE]}^*$	$\rho_{[I_i/FE]}^*$	$\rho_{[I_{i-1}/EX]}$	$\rho_{[I_{i-2}/EX]}$
EX	$\rho_{[I_{i-1}/EX]}$	$\rho_{[I_{i-1}/EX]}^*$	$\rho_{[I_{i-2}/EX]}^*$	$\rho_{[I_i/DE]}^*$	$\rho_{[I_{i-1}/ME]}$	$\rho_{[I_{i-2}/ME]}$
ME	$\rho_{[I_{i-1}/CM]}$	$\rho_{[I_{i-1}/ME]}^*$	$\rho_{[I_{i-2}/ME]}^*$	$\rho_{[I_i/EX]}^*$	$\rho_{[I_{i-1}/CM]}$	$\rho_{[I_{i-2}/CM]}$
CM	$\rho_{[I_{i-1}/ME]}$	$\rho_{[I_{i-1}/CM]}^*$	$\rho_{[I_{i-2}/CM]}^*$	$\rho_{[I_i/ME]}^*$	$-\infty$	$-\infty$
	Fetch Order	Memory Order		Data Dependencies		
FE	$\rho_{[I_{fetch}/FE]}^*$	$-\infty$		$-\infty$		
DE	$-\infty$	$-\infty$		$-\infty$		
EX	$-\infty$	$-\infty$		$\rho_{[I_{R0}/s_{R0}]}^*$	$\rho_{[I_{R0}/s_{R1}]}^*$	\dots
ME	$-\infty$	$\rho_{[I_{load}/ME]}^*$	$\rho_{[I_{store}/ME]}^*$	$\rho_{[I_{R0}/s_{R0}]}$	$\rho_{[I_{R1}/s_{R1}]}$	\dots
CM	$-\infty$	$-\infty$		$-\infty$		

release time of all dependencies which is the actual start time for the analyzed XG vertex. The transitions for the *temporal state* are defined with the functions τ_{reset} and τ_{wait} :

$$\tau_{reset} : \mathcal{S} \rightarrow \mathcal{S},$$

$$\tau_{reset}(\vec{S}) = \vec{S}' \mid \begin{cases} \vec{S}'[i] = \vec{S}[i] \otimes \mathbb{0} & \text{if } i = i_\varrho \\ \vec{S}'[i] = \vec{S}[i] & \text{otherwise} \end{cases} \quad (7)$$

$$\tau_{wait} : \mathbb{N} \times \mathcal{S} \rightarrow \mathcal{S},$$

$$\tau_{wait}(x, \vec{S}) = \vec{S}' \mid \begin{cases} \vec{S}'[i] = \vec{S}[i] \oplus \vec{S}[x] & \text{if } i = i_\varrho \\ \vec{S}'[i] = \vec{S}[i] & \text{otherwise} \end{cases} \quad (8)$$

τ_{wait} has to be called for each dependency (with index x in the *temporal state* vector) of the current vertex.

- Step 2. Some resources (e.g. the Queues between stages) are released at the start of an XG vertex. The corresponding dependencies (Queue Capacity) have to be updated with the start time ρ recorded by the time pointer ϱ .

Generally, the update of the vector is done with τ_{move} :

$$\tau_{move} : \mathbb{N} \times \mathbb{N} \times \mathcal{S} \rightarrow \mathcal{S},$$

$$\tau_{move}(i_{dest}, i_{src}, \vec{S}) = \vec{S}' \mid \begin{cases} \vec{S}'[i] = \vec{S}[i_{src}] & \text{if } i = i_{dest} \\ \vec{S}'[i] = \vec{S}[i] & \text{otherwise} \end{cases} \quad (9)$$

τ_{move} copies a vector element into another element and overwrites the destination value. Updating the dependency of a single resource amounts to copying ϱ into the slot of the dependency: for example, updating the state of a dependency d of index i_d with the start time (recorded in the time pointer ϱ) consists in $\tau_{move}(i_d, i_\varrho, \vec{S})$. The state of FIFO resources (like queues) requires updating several *temporal state* slots (i to $i + n - 1$ with n the FIFO capacity) to express the shift of the n last FIFO

uses. Hence FIFO resources are updated by a series of τ_{move} on the n FIFO slots in the *temporal state* and by setting the first slot to ϱ , the use time for the first FIFO element:

$$\forall j \in [i, i + n - 2], \tau_{move}(j + 1, j, \vec{S});$$

$$\tau_{move}(i, i_\varrho, \vec{S});$$

- Step 3. The started instruction spends $\lambda_{[I_i/s]}$ cycles in the stage. After this step, the value the time pointer is the end time of $[I_i/s]$.

$$\tau_{consume} : \mathbb{N} \times \mathcal{S} \rightarrow \mathcal{S},$$

$$\tau_{consume}(\lambda_{[I_i/s]}, \vec{S}) = \vec{S}' \mid \begin{cases} \vec{S}'[i] = \vec{S}[i] \otimes \lambda_{[I_i/s]} & \text{if } i = i_\varrho \\ \vec{S}'[i] = \vec{S}[i] & \text{otherwise} \end{cases} \quad (10)$$

- Step 4. The instruction finishes its execution and the dependencies recording the end time of the current vertex are updated. The τ_{move} operation is used in the same way as in the Step 2.

As in the original XG resolution model, the computational model with *temporal states* has to follow the topological order so that the times recorded in the XDD vector refer to the correct timing of resources. In other words, if the state is correctly updated according to the rules stated above, the resource-based model is equivalent to the original XG analysis but expressed in state machine fashion. The implementation using XDDs extends the model to consider all possible cases according to the timing variations without any loss. The BB analysis is consequently *exact* with respect to the XG pipeline model.

C. The computational model

An important property of the XDD domain is that, equipped with \oplus and \otimes , it forms the semiring $(\text{XDD}, \oplus, \otimes, \mathbb{0}, \mathbb{1})$ with $\mathbb{0} = \text{LEAF}(-\infty)$ and $\mathbb{1} = \text{LEAF}(0)$. As the transition

functions τ are affine in this domain, their application can be expressed as matrix multiplications. Combining and pre-computing these matrices will help to speed up the pipeline analysis at CFG level since some BBs need to be recomputed several times in different execution contexts.

Scalar and matrix multiplication on XDD semiring is similar to the linear algebra over \mathbb{R} by replacing $+$ by \oplus , \times by \otimes :

Definition IV.2. The scalar multiplication is defined by:

$$\begin{aligned} \cdot : \text{XDD}^N \times \text{XDD}^N &\rightarrow \text{XDD}, \\ [f_0, f_1, \dots, f_{N-1}] \cdot [f'_0, f'_1, \dots, f'_{N-1}] &= \bigoplus_{0 \leq i \leq N-1} f_i \otimes f'_i \end{aligned}$$

Definition IV.3. The matrix multiplication is defined by:

$$\begin{aligned} \cdot : \text{XDD}^{N \times M} \times \text{XDD}^{M \times L} &\rightarrow \text{XDD}^{N \times L}, \\ B \cdot C &= \left[\begin{array}{c} A_{i,j} \end{array} \right] | A_{i,j} = \bigoplus_{1 \leq k \leq M} B_{i,k} \otimes C_{k,j} \end{aligned}$$

Definition IV.4. The identity matrix Id on the XDD semiring is defined by:

$$Id = \left[\begin{array}{c} A_{i,j} \end{array} \right] | A_{i,j} = \begin{cases} \mathbb{1} & \text{if } i = j \\ \mathbb{0} & \text{otherwise} \end{cases}$$

Note that, by definition, $\vec{S} \cdot Id = \vec{S}$: any matrix column at index i contains only $\mathbb{0}$ except for the row i that contains a $\mathbb{1}$, which maintains unchanged the value of $\vec{S}[i]$ in the resulting vector. To implement the transition functions τ as matrix multiplications, the matrix Id is taken as a basis and only the cells that have an effect on the vector have to be changed.

- 1) A $\mathbb{0}$ on the diagonal of the Id matrix at the timer pointer position resets it: $\vec{S}[i_\rho] \otimes \mathbb{0} = \mathbb{0}$:

$$\begin{aligned} \tau_{reset}(\vec{S}) &= \vec{S} \cdot M_{reset} \\ &= \vec{S} \cdot \left[\begin{array}{c} A_{i,j} \end{array} \right] | A_{i,j} = \begin{cases} \mathbb{0} & \text{if } i = j = i_\rho \\ Id_{i,j} & \text{otherwise} \end{cases} \end{aligned} \quad (11)$$

- 2) For a given slot at index x in \vec{S} , $\tau_{wait}(x, \vec{S})$ is represented by a matrix $M_{wait(x)}$ with a $\mathbb{1}$ at position (x, i_ρ) resulting in the operation $\rho \oplus (\mathbb{1} \otimes \vec{S}[x])$:

$$\begin{aligned} \tau_{wait}(x, \vec{S}) &= \vec{S} \cdot M_{wait(x)} \\ &= \vec{S} \cdot \left[\begin{array}{c} A_{i,j} \end{array} \right] | A_{i,j} = \begin{cases} \mathbb{1} & \text{if } i = i_\rho \wedge j = x \\ Id_{i,j} & \text{otherwise} \end{cases} \end{aligned} \quad (12)$$

- 3) $\tau_{move}(i_{src}, i_{dest}, \vec{S})$ is represented by a matrix $M_{move(i_{src}, i_{dest})}$ where the element at (i_{dest}, i_{dest}) is set to $\mathbb{0}$ and the element (i_{dest}, i_{src}) to $\mathbb{1}$ s.t. element i_{dest} in the result becomes $(\mathbb{0} \otimes \vec{S}[i_{dest}]) \oplus (\mathbb{1} \otimes \vec{S}[i_{src}]) = \vec{S}[i_{src}]$.

$$\begin{aligned} \tau_{move}(i_{src}, i_{dest}, \vec{S}) &= \vec{S} \cdot M_{move(i_{src}, i_{dest})} \\ &= \vec{S} \cdot \left[\begin{array}{c} A_{i,j} \end{array} \right] | A_{i,j} = \begin{cases} \mathbb{0} & \text{if } i = j = i_{dest} \\ \mathbb{1} & \text{if } i = i_{dest} \wedge j = i_{src} \\ Id_{i,j} & \text{otherwise} \end{cases} \end{aligned} \quad (13)$$

- 4) For a given latency λ , $\tau_{consume}(\lambda, \vec{S})$ can be represented by a matrix $M_{consume(\lambda)}$, obtained from Id by putting λ at position (i_ρ, i_ρ) .

$$\begin{aligned} \tau_{consume}(\lambda, \vec{S}) &= \vec{S} \cdot M_{consume}^\lambda \\ &= \vec{S} \cdot \left[\begin{array}{c} A_{i,j} \end{array} \right] | A_{i,j} = \begin{cases} \lambda & \text{if } i = j = i_\rho \\ Id_{i,j} & \text{otherwise} \end{cases} \end{aligned} \quad (14)$$

Theorem IV.1. Each transition function τ applied to the timing vector is a linear map from \mathcal{S} to \mathcal{S}

Proof. Direct since we have already given the matrix representation of each transition in Definition IV.4. \square

Consequently, the operations performed at each step are also linear because they are combination of τ functions. Their matrix representation is simply the multiplication of each invoked τ function. For example,

$$M_{Step_1[I_i/s]} = M_{reset} \cdot \prod_{d \in \mathcal{D}_{[I_i/s]}} M_{wait(i_d)}$$

with $\mathcal{D}_{[I_i/s]}$ the set of dependencies required by $[I_i/s]$ and i_d the index of resource d in the state vector.

Similarly, we can express $M_{Step_2[I_i/s]}$, $M_{Step_3[I_i/s]}$ and $M_{Step_4[I_i/s]}$ by invoking the corresponding τ functions. As each step is linear, the operation when analyzing one instruction on a stage is also linear because it is the combination of the 4 steps.

$$M_{[I_i/s]} = M_{Step_1[I_i/s]} \cdot M_{Step_2[I_i/s]} \cdot M_{Step_3[I_i/s]} \cdot M_{Step_4[I_i/s]}$$

Finally, the whole analysis of a BB $a \in V$ is composed by the analysis of each instruction in each pipeline stage:

$$M_a = \prod_{I_i \in a} \prod_{s \in \mathcal{P}} M_{[I_i/s]}$$

With a matrix such as M_a , it is easy and fast to compute the output temporal state $\vec{S}' \in \mathcal{S}$ corresponding to an input temporal state $\vec{S} \in \mathcal{S}$ for a BB a :

$$\vec{S}' = \vec{S} \cdot M_a \quad (15)$$

V. PIPELINE ANALYSIS ON THE CFG

This section extends the *temporal state* computational model, presented in the previous section, to the complete analysis of the CFG. It mainly consists in tracking the explicit set of possible temporal states for each BB all over the CFG execution paths.

A. Computing the context with Rebasing operation

In an analysis at BB-level, a temporal state contains times relative to the start of a BB. In an analysis at CFG-level, a temporal state should contain times relative to the start of the program and the temporal states should be tracked for all possible execution paths. This is generally infeasible because of the huge number of execution paths, especially in the presence of loops.

Now the main reason for which we want to compute exact temporal states at CFG-level is to determine the exact timings of bus accesses. But these timings do not need to be absolute with respect to the start of the program. Instead, they can be relative to arbitrarily-chosen time bases, as long as XDDs with different bases are not mixed.

We call *rebasing* the operation that consists in changing the origin of the timeline of a temporal state. The temporal state at the end of BB a represents the delay induced by the execution of a to the start of the following BB b . Considering the start of b as a new time base $T \in \text{XDD}$, we can get a new temporal state relative to T by subtracting T from the times in the temporal state in the base of BB a . The outcome is a temporal state containing XDDs with positive or negative times relative to T . The relationship between times and events in the temporal state is preserved. The subtraction in XDDs \ominus is built in the usual way from the $-$ operator (Eq. (3)).

Rebasing a temporal state is lossless because \ominus is reversible. By adding T (with \otimes), one can find back the state before rebasing. Rebasing is very helpful to reduce the size of XDDs in the temporal state: an event removed by rebasing has no effect on the following BBs but it does not mean it has no effect at all. Its contribution to the overall WCET is simply linear with respect to the number of occurrences of the BB. Intuitively, the execution of an instruction depends on the execution of nearby instructions. Thus the effect of events is generally short term and is, in practice, often eliminated by rebasing.

B. Generation of Events within loops

Each event computed by global analyses is linked to a particular instruction. The pipeline analysis of a BB presented so far deems the occurrence of events unique. This is not true when an event arises in a BB of a loop body, since it may occur or not in different iterations. We would get unsound timings if we denoted these different event occurrences with the same event node in the XDD. To fix this, a *generation number* is associated with each event. To prevent a blowup of temporal states, this generation number is relative to the current iteration and is incremented in the current temporal state each time the analysis iterates in the loop. The generation number thus distinguishes occurrences of an event in different iterations. Fortunately, this method does not result in an endless increase of generations because (a) the effect of events is often bounded in time and (b) the WCET calculation requires to bound the number of loop iterations.

C. The CFG pipeline analysis

Finally, the complete pipeline analysis is designed like a classical data-flow analysis with a work list. Each BB is associated with a set of input temporal states and a set of output temporal states (initially empty). The analysis starts with an initial temporal state at the entry of the CFG and propagates the new states all along the CFG paths. For each entry edge of a BB, the input state set is the union of the output states of the preceding BBs. Each input state is updated (i.e. multiplied by the pre-computed matrix) and rebased to make a new output state. If the set of its output states differs from the original set, the successors of the BB are pushed into the work list. The process is repeated until finding a fix-point on all sets of input/output states has been reached. For readers familiar with abstract interpretation, this is actually the *collecting semantics* of our pipeline semantics.

Using XDD, the variability caused by events is efficiently recorded without any loss thanks to its *compaction* property. Besides, the analysis at CFG-level collects the set of all possible pipeline states, meaning it is also lossless according to the variability caused by the control-flow. In turn, this means that the resulting set of vectors of XDDs contains sufficient information to determine the exact temporal behavior of each BB in all possible situations. They can then be used to precisely analyze the temporal behavior in presence of out-of-order scheduled resources.

VI. MODELING THE SHARED MEMORY BUS

In previous work, our analysis was valid only when all the resources were accessed in the program order. However, in embedded microprocessors, the instruction and data caches often share a common bus to the memory (or to a unified L2 cache). This introduces an out-of-order behavior: an instruction cache miss might access the shared bus before a data cache miss generated by an older instruction. In other words, the variability due to events in the start times of the FE and ME nodes may change the access order to the shared bus. Since XG dependencies are not expressive enough to model out-of-order bus allocations, we propose, in this section, an extension to the pipeline analysis to efficiently manage the shared bus accesses according to the different configurations of the temporal states. It supports the usual bus arbitration policy: first-come-first-served (FCFS), with priority given to the ME stage in case of simultaneous bus accesses.

A. Bus scheduling properties

Since we consider an in-order pipeline, the number of possible contention scenarios on the shared bus is limited. For instance, an instruction using the bus in the ME stage cannot contend with any subsequent instructions in the ME stage (load/store memory order is preserved). Similarly, bus accesses by the FE stage follow the program order. Moreover, the pipeline order ensures that a request emitted by an instruction in the FE stage is granted the bus before a request emitted by the same instruction in the ME stage. This means that the bus allocation in an in-order pipeline is almost completely in-order,

TABLE III: Possible schedules of ME_0 with subsequent FEs .

Schedule	Condition	Scheduling time of ME_0
ME_0, FE_1, FE_2, FE_3	$\rho_{ME_0} \leq \rho_{FE_1}$	ρ_{ME_0}
FE_1, ME_0, FE_2, FE_3	$\rho_{FE_1} < \rho_{ME_0} \leq \rho_{FE_2}$	$\max(\rho_{FE_1} + \lambda_{BUS}, \rho_{ME_0})$
FE_1, FE_2, ME_0, FE_3	$\rho_{FE_2} < \rho_{ME_0} \leq \rho_{FE_3}$	$\max(\rho_{FE_2} + \lambda_{BUS}, \rho_{ME_0})$
FE_1, FE_2, FE_3, ME_0	$\rho_{FE_3} < \rho_{ME_0}$	$\max(\rho_{FE_3} + \lambda_{BUS}, \rho_{ME_0})$

with only one exception: a bus request in the ME stage by an instruction denoted ME_0 may be delayed by a bus request in the FE stage by a younger instruction denoted $FE_{i|i>0}$. To simplify the notation in this section, ME_0 and $FE_{i|i>0}$ denote the instructions as well as the XG vertex (e.g. ME_0 also denotes vertex $[ME_0/ME]$; FE_1 also denotes $[FE_1/FE]$). In-between instructions are disregarded but are still accounted for in the matrices used to update the temporal states.

To sum up, FE_i can delay ME_0 only if FE_i is ready to enter FE stage before ME_0 is ready to enter ME. In the XG model, this situation can only happen when FE_i does not depend on ME_0 , that is, when there is no path from ME_0 to FE_i ³.

In the example of Table III, we consider that ME_0 can only be delayed by FE_1 , FE_2 and FE_3 . For a particular configuration of events, there are four possible schedules that are shown in the first column of the table. These four schedules correspond to the four possible ways to interleave ME_0 with FE_i accesses. The actual schedule is determined by comparing the ready time of ME_0 (ρ_{ME_0}) with the ready times of FE_1 , FE_2 and FE_3 (resp. ρ_{FE_1} , ρ_{FE_2} and ρ_{FE_3}): the second column shows the condition corresponding to each schedule. The third column gives the actual time at which ME_0 gets the bus with λ_{BUS} denoting the latency of a bus access (including the memory transaction): if ME_0 is the first to be ready, then it gets the bus at time ρ_{ME_0} . Otherwise, ME_0 gets the bus at the maximum time between its ready time and the release time of bus by the FE_i contender.

B. Batch bus scheduling with XDD

Table III shows the schedule of ME_0 for a given configuration. However, when times are expressed as XDDs, a particular XDD may support configurations with different bus schedules. That said, we must extend the computation of the condition and the scheduling time in order to support XDDs. Figure 3 shows such an example in a simpler scenario: ME_0 may be delayed by FE_1 and FE_2 . Let us assume their start date without counting the contention (ρ_{S_i}) as shown in the figure. The objective is to compute the actual start dates of ME_0 and FE_i with contention ($\hat{\rho}_{ME_0}$ and $\hat{\rho}_{FE_i}$). The instruction fetch in FE_1 may result in a cache hit or a cache miss, which is represented by event ic_1 . The instruction fetch in FE_2 is assumed to be classified as Always Miss, meaning that it always requests the bus. The latency of a bus access is assumed to be 9 cycles. The events e_0 and e_1 are events

³The occurrence of such situations is limited by the size of the inter-stage queues in the pipeline.

related to the instructions before ME_0 that are assumed to impact the start time of ME_0 and FE_2 .

XDD (a) shows the ready time of ME_0 and (b) the initial value of $\hat{\rho}_{ME_0}$ – the scheduling time of ME_0 on the bus ($+\infty$ means that no access is yet scheduled). (c) shows the initial value of ρ_{rel} , recording the release time of the bus by FE_i ($-\infty$ denotes that the bus is not used by any FE_i for now).

The ready time of FE_1 (d) is computed from the initial state \vec{S}_0 and the matrix between ME_0 and FE_1 . The event ic_1 indicates with $-\infty$ the configuration where FE_1 does not use the bus (hence it is not concerned by the contention).

ρ_{ME_0} (a) and ρ_{FE_1} (d) are compared using \blacktriangleleft_{ME} to get the configurations and the time ($\rho_{schedME_0}$ (e)) when ME_0 takes the bus, i.e. is scheduled, before FE_1 (\blacktriangleleft_{ME} is formally defined in Eq. (16)). Other configurations are assigned $+\infty$, denoting that they are not processed yet. Notice that a $-\infty$ configuration in ρ_{FE_i} does not allow ME_0 to be scheduled as subsequent $FE_{j>i}$ might allocate the bus before ME_0 . $\rho_{schedME_0}$ is then used to update $\hat{\rho}_{ME_0}$ using the minimum operator \ominus (f).

$\rho_{schedFE_1}$ (g), i.e. the configurations where FE_1 gets the bus, is computed in a similar way as $\rho_{schedME_0}$ but with operator \blacktriangleleft_{FE} that selects the configurations in which FE gets the bus, using the strict $<$ comparison instead of \leq because the ME stage has priority over the FE stage in case of simultaneous requests. By adding the latency of the bus (λ_{BUS}) to $\rho_{schedFE_1}$, we are able to update, using \oplus , the release time of the bus after FE_1 (ρ_{rel} (h)). Finally, we compute the actual schedule of FE_1 ($\hat{\rho}_{FE_1}$ (i)) that is the time of $\rho_{schedFE_1}$ if FE_1 is scheduled, or otherwise the release time of the bus by ME_0 ($\hat{\rho}_{ME_0} \otimes \lambda_{BUS}$). Now, as the actual schedule of FE_1 is known, the release time of the bus at FE_1 is computed and is used to adjust the *temporal state*. By multiplying the state \vec{S}_{FE_1} by the matrix $M_{FE_1-FE_2}$, we get the ready time of FE_2 (j). In the second iteration, first, ρ_{ME_0} (a) is compared with ρ_{FE_2} (j) with the operator \blacktriangleleft_{ME} . The actual scheduling time $\rho_{schedME_0}$ (k) is computed by considering the maximum between $\rho_{schedME_0}$ and the release time of the bus by FE_1 (ρ_{rel}) according to the third column of Table III. Then, $\hat{\rho}_{ME_0}$ is updated (l). The schedule of FE_2 – $\rho_{schedFE_2}$ (m) is computed with the operator \blacktriangleleft_{FE} applied to ρ_{FE_2} and ρ_{ME_0} which is then used to update the release time of the bus ρ_{rel} (n). The actual schedule of FE_2 is computed with respect to the use of the bus by ME_0 (o).

When the end of the sequence is reached, there are no further subsequent instructions that may contend with ME_0 and the remaining $+\infty$ in $\hat{\rho}_{ME_0}$ represents configurations

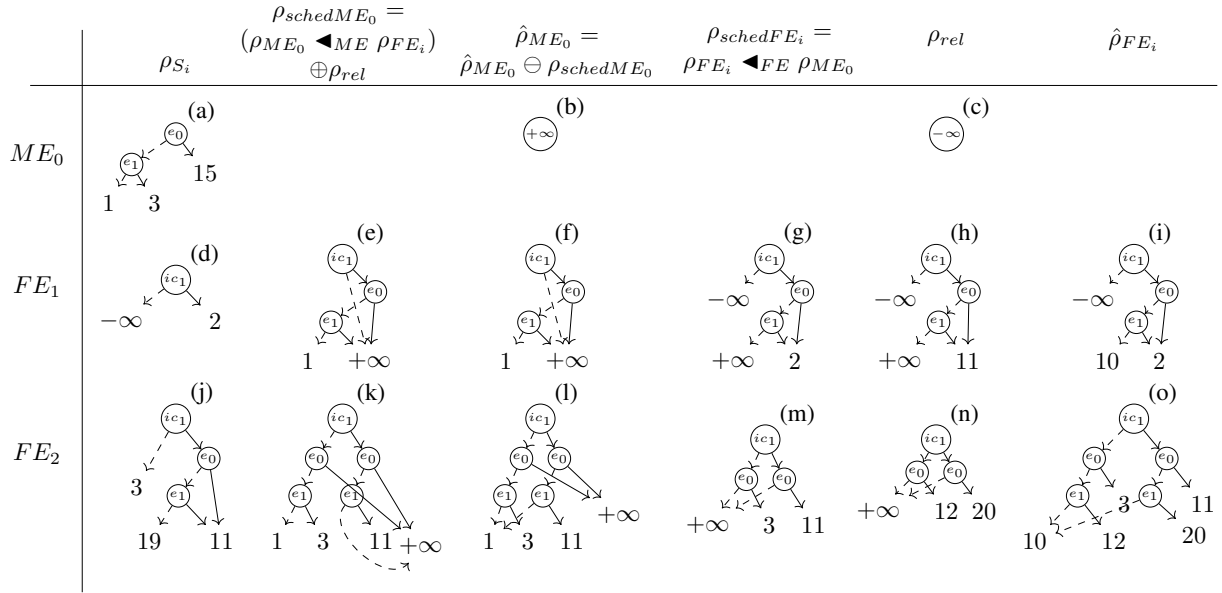


Fig. 3: Batch bus scheduling with XDDs.

accessing the bus after FE_1 and FE_2 . They are replaced by the maximum between the ready time of ME_0 and the release times of the bus by FE_1 and FE_2 , ρ_{rel} .

Operator \blacktriangleleft_{ME} (resp. \blacktriangleleft_{FE}) has a straightforward definition, setting to $+\infty$ the configurations where ME (resp. FE) does not get the bus:

$$\forall f_{ME}, f_{FE} \in \text{XDD}^2, \forall \gamma \in \Gamma,$$

$$(f_{ME} \blacktriangleleft_{ME} f_{FE})[\gamma] = \begin{cases} f_{ME}[\gamma] & \text{if } f_{ME}[\gamma] \leq f_{FE}[\gamma], \\ +\infty & \text{otherwise} \end{cases}$$

$$(f_{FE} \blacktriangleleft_{FE} f_{ME})[\gamma] = \begin{cases} f_{FE}[\gamma] & \text{if } f_{FE}[\gamma] < f_{ME}[\gamma], \\ +\infty & \text{otherwise} \end{cases} \quad (16)$$

All these calculations seem a bit complex but it must be kept in mind that real XDDs are much more complex with much more configurations and relying on the XDD operators allows to benefit from the XDDs optimizations.

C. Contention Analysis

The contention analysis depicted in the previous example is described more formally in this paragraph. Basically, the pipeline analysis is extended by splitting the BBs at *contention points*, i.e. at the XG nodes where a bus access may occur (ME or FE stages causing cache misses). Then they are grouped in a sequence of one ME access followed by zero or several FE accesses, $(ME_0, FE_{0 < i \leq n})$. The instructions between two successive *contention points* are summarized by a pre-computed matrix.

Algorithm 1 is then applied to compute the possible interleaving of bus accesses for all configurations of the sequence $(ME_0, FE_{0 < i \leq n})$. Additionally, it takes as input the *temporal state* \vec{S}_0 . The result is the definitive schedule of ME_0 (i.e. $\hat{\rho}_{ME_0}$) and of FE_i (i.e. $\hat{\rho}_{FE_i}$).

Algorithm 1: Contention computation.

Input: $\vec{S}_0 \in \mathcal{S}, (ME_0, FE_{1 \leq i \leq n})$
Output: $(\hat{\rho}_{ME_0}, \hat{\rho}_{FE_{1 \leq i \leq n}})$

- 1 $\hat{\rho}_{ME_0} = \text{LEAF}(+\infty)$
- 2 $\rho_{rel} := \text{LEAF}(-\infty)$
- 3 $\vec{S}_{FE_1} := \vec{S}_{ME_0} \cdot M_{ME_0 - FE_1}$
- 4 $i := 1;$
- 5 $\rho_{ME_0} := \vec{S}_0[i_\rho]$
- 6 **while** $i \leq n \wedge (\exists \gamma \in \Gamma \wedge \hat{\rho}_{ME_0}[\gamma] = +\infty)$ **do**
- 7 **if** $FE_i.\text{mustUseBus}()$ **then**
- 8 $\rho_{FE_i} := \vec{S}_{FE_i}[i_{FE}]$
- 9 **else**
- 10 $\rho_{FE_i} := \vec{S}_{FE_i}[i_{FE}] \otimes \text{NODE}(ic_i, -\infty, 0)$
- 11 $\rho_{schedME_0} := (\rho_{ME_0} \blacktriangleleft_{ME} \rho_{FE_i}) \oplus \rho_{rel}$
- 12 $\hat{\rho}_{ME_0} := \hat{\rho}_{ME_0} \ominus \rho_{schedME_0}$
- 13 $\rho_{schedFE_i} := \rho_{FE_i} \blacktriangleleft_{FE} \rho_{ME_0}$
- 14 $\rho_{rel} := \rho_{rel} \oplus (\rho_{schedFE_i} \otimes \lambda_{BUS})$
- 15 $\hat{\rho}_{FE_i} := \rho_{schedFE_i} \ominus (\hat{\rho}_{ME_0} \otimes \lambda_{ME_0})$
- 16 $\vec{S}_{FE_{i+1}} :=$
 $(\vec{S}_{FE_i} \oplus [\mathbf{0}, \dots, \mathbf{0}, \hat{\rho}_{FE_i} \otimes \lambda_{BUS}]) \cdot M_{FE_i - FE_{i+1}}$
- 17 $i = i + 1$
- 18 $\hat{\rho}_{ME_0} := \hat{\rho}_{ME_0} \ominus (\rho_{rel} \oplus \rho_{ME_0})$

Initially, ME_0 is considered as not scheduled whatever the considered configuration and $\hat{\rho}_{ME_0}$ is set to $\text{LEAF}(+\infty)$ (line 1). It will then be updated after considering the contention with each subsequent FE_i . When ME_0 does not contain $+\infty$ anymore or when all FE_i have been processed, the schedule of ME_0 is complete (condition at line 6). Line 2 initializes ρ_{rel} that records the release time of the bus by FE_i to $-\infty$

as no FE_i has been processed yet.

In line 3, the *temporal state* just before FE_1 is computed by applying the matrix $M_{ME_0-FE_1}$ to the initial state \vec{S}_0 ; i is initialized in line 4 and will range over the *Contention Points*, 1 to n . The ready time of ME_0 is recorded into ρ_{ME_0} at line 5. Lines 7-10 compute the ready time of FE_i if the access always or sometimes results in a miss (according to *mustUseBus()*). The latter case is expressed by the event ic_i and by adding the $NODE(ic_i, -\infty, 0)$ to ρ_{FE_i} : $-\infty$ denotes the case where ic_i does not arise and there is no bus access.

$\rho_{schedME_0}$, ME_0 configurations getting the bus before FE_i , is computed with \blacktriangleleft_{ME} at line 11 by comparing the ready times of ME_0 with the ones of FE_i . According to the last column of Table III, these configurations are fixed by taking the maximum between the ready time of ME_0 and the release time of the bus ρ_{rel} . The schedule of ME_0 at this iteration is accumulated in the definitive schedule of ME_0 at line 12. At line 13, the schedule of FE_i is computed. Notice that as the ready time of FE_i contains $-\infty$ to denote the case where it does not use the bus, these $-\infty$ are kept in $\rho_{schedFE_i}$. By adding the bus latency λ_{BUS} to $\rho_{schedFE_i}$ and then \oplus with ρ_{rel} , the release time of the bus is only updated for configurations γ where FE_i uses and gets the bus ($\rho_{schedFE_i}[\gamma] \neq +\infty$) (line 14). Notice that the $+\infty$ in ρ_{rel} cannot overwrite the release time of the bus by FE_i because FE_i cannot get the bus if any prior $FE_{j<i}$ does not get the bus. At line 15, the actual schedule of FE_i is computed by replacing the $+\infty$ in $\rho_{schedFE_i}$ (where FE_i loses contention in favor of ME_0) by the release time of the bus by ME_0 . Configurations where time is $+\infty$ in $\rho_{schedFE_i}$ must not be $+\infty$ in $\hat{\rho}_{ME_0}$ because only one of FE_i or ME_0 is scheduled. However, as $\rho_{schedFE_i}$ configurations not leading to $+\infty$ are lower than $\hat{\rho}_{ME_0}$ (otherwise it is considered as non-scheduled), \ominus can be used to implement the replacement.

At line 16, the *temporal state* is updated regarding the schedules of FE_i , by applying \oplus between the time pointer of the state vector and the release time of the bus by FE_i . The updated state is then multiplied by matrix $M_{FE_i-FE_{i+1}}$ to obtain the ready time of FE_{i+1} . Line 18 takes into account the remaining $+\infty$ configurations in $\hat{\rho}_{ME_0}$ that are not already scheduled by the loop. The times assigned to these configurations are the maximum between the ready time of ME_0 and the bus release time by FE_i . Notice that $+\infty$ in the $\hat{\rho}_{ME_0}$ may also be caused by the fact that none of the FE_i have used the bus: this time is recorded as $-\infty$ in ρ_{rel} and is hence automatically overwritten by the ready time of ME_0 .

VII. EVALUATION

The performance of the analysis strongly depends on the size of the XDDs in the pipeline states and on the number of pipeline states. Both metrics are related to some inherent properties of the analyzed program and of the micro-architecture, the impact of which is difficult to theoretically estimate. Therefore, we experiment our analysis on realistic benchmarks that empirically provide a better understanding of the performance.

A. Experimental Setup

The pipeline used in the examples of the previous sections was chosen to enhance the readability of the article. For the experimentation, we consider a more powerful micro-architecture with more parallelism leading to more complex temporal states. In addition, this new pipeline allows demonstrating the scalability of our approach.

Our pipeline has 4 stages (FE, DE, EX, CM), each able to process 4 instructions per cycle. In the FE stage, it fetches instructions from a single-level instruction cache. The FE stage is able to fetch 4 instructions of the same memory block simultaneously, with a latency of 7 cycles in case of a cache miss (ignoring possible contention). The DE stage decodes the instructions and the EX stage handles all arithmetic, floating point and memory related operations in several functional units (FU). Four ALUs (Arithmetic and Logic Units) are available and can be simultaneously used by independent instructions. The latency of arithmetic operations is 1 cycle for additions and subtractions, 2 cycles for multiplications and 7 cycles for divisions. One FPU (Floating Point Unit) is available with a latency of 3 cycles for additions and subtractions, 5 cycles for multiplications and 12 cycles for divisions. A single MU (Memory Unit) handles memory-related operations (loads and stores). In case of a multiple load/store operation, the memory accesses are performed in order, and if one multiple load/store needs to use the memory bus (in case of data cache misses), it occupies it until all loads/stores are completed. The latency of data accesses is the same as for instruction fetches. In the EX stage, an issue buffer distributes the instructions to the appropriate FUs. Instructions using the same FU are executed in order; instructions using different FUs can be executed out-of-order (if the absence of data dependencies).

The instruction cache is a 16-KByte 2-way set associative LRU (Least Recent Used) cache. The data cache is a 8-KByte 2-way set associative LRU cache. There is a single level of caches and they share the same bus to the main memory. We believe that this architecture is representative of many mid-range processors used in real-time embedded systems.

The whole CFG analysis is implemented using the OTAWA toolbox [11]. Global analyses, including instruction and data cache analyses as well as control flow analyses are provided by OTAWA. The benchmarks are taken from the TACLe suite [10] compiled for the armv7 instruction set with a hard floating point unit. Among 79 tasks to be analyzed, 5 fail due to limitations in OTAWA (unsupported irregular control flow⁴, e.g. unable to solve dynamic branch address) and another 5 have been dropped due to the lack of annotations on the bounds of recursive function calls⁵, for which the WCET computation is impossible.

B. Number of Temporal States

The first experiment explores the number of temporal states along the edges of BBs (representing the output of the source

⁴*pm, mpeg2, gsm_enc, ammunition, rosace*

⁵*recursion, huff_enc, quicksort, bitonic, anagram*

BBs and the input of sink BBs). The experimental results are shown in Figure 4. The x-axis shows the number of pipeline states and the y-axis shows the number of edges for each amount of states (in a logarithmic scale). The bars accumulate data from all the benchmarks.

The risk, with our approach at CFG level, is to face an exploding number of states which is a common concern of collecting semantic based analyses. Fortunately, the experimentation shows that most of the edges have less than 20 output states. This means that most of the timing variations due to events are efficiently represented in the XDDs of the temporal states. As expected, the XDDs successfully prevent the state explosion and keep the pipeline analysis tractable at CFG-level. The presence of some rare cases where the number of states is much higher is not blocking as the analysis time remains reasonable in most cases (cf. Section VII-D).

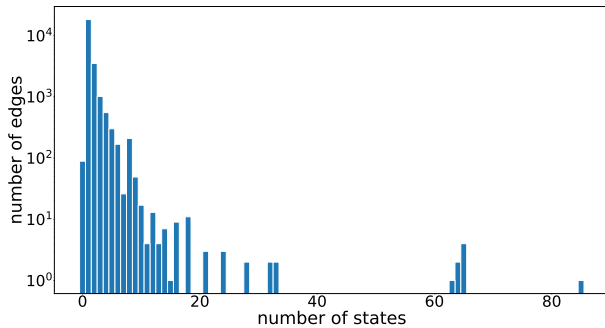


Fig. 4: The distribution of number of pipeline states.

C. Events Lifetime

The second experiment measures the lifetime of events during the analysis. The longer the lifetime of events, the larger the complexity of the analysis in terms of number of states and size of XDDs. In our micro-architecture, an event is created by a cache access and may disappear from the XDD during the analysis, for two reasons: (i) it is absorbed by the pipeline: for example, when an instruction stalls in the EX stage due to a data cache miss, the next instructions may still be processed in the pipeline, completely hiding the stalling time – this event will stay alive only in a short time window during the analysis of other instructions executed in parallel. (ii) The events are *stabilized* and disappear thanks to the rebasing operation. Intuitively, we assume that in most situations, the events raised by an instruction only impact nearby instructions. Therefore, the lifetime of events provides a fine estimation of both the size of XDDs and the number of pipeline states of our analysis at CFG-level. As complement, in [2], we provide detailed discussion and experiments, on different micro-architecture setups, of the size of XDDs for BB-level analysis where the pipeline absorption effect is the primary factor.

However, the pipeline analysis is only able to provide the lifetime information at the granularity of *contention points* because the effect of executing instructions between contention points is expressed by matrices. As collecting these statistics at a finer granularity would have an important adverse effect

on the analysis time, we survey the liveness of events on this basis. Events are deemed as dead at contention points if the temporal state of which does not contain the event in any XDD contained in the vector. Thus, the lifetime statistics are over-estimated by the number of instructions between contention points. Besides, the pipeline states are only rebased at the end of BBs so the lifetime of events in the middle of BBs does not consider the potential death due to rebasing. In the end, the measured lifetime in this experimentation is an over-estimation of the actual lifetime of events.

Figure 5 shows the experimental results. The x-axis is the lifetime of events (in instructions with limitations described above) and the y-axis, in logarithm scale, shows the number of events having this lifetime. These are also accumulated from the whole set of TACLe benchmarks. The statistics show that most events have a short lifetime (below 50 instructions). We have observed a unique lifetime of 602 instructions that is not represented to keep the figure readable. It turns out that in most situations where the lifetime is greater than 50, the events are in a very long BB. In the extreme case of the 602-instruction event lifetime, the involved BB contains 617 instructions (in benchmark *md5*) and the reported lifetime is an effect of the granularity level. Despite this very infrequent case, most events have short lifetimes and the size of temporal states (sum of XDDs sizes of the vector) is reasonable and the analysis remains efficient.

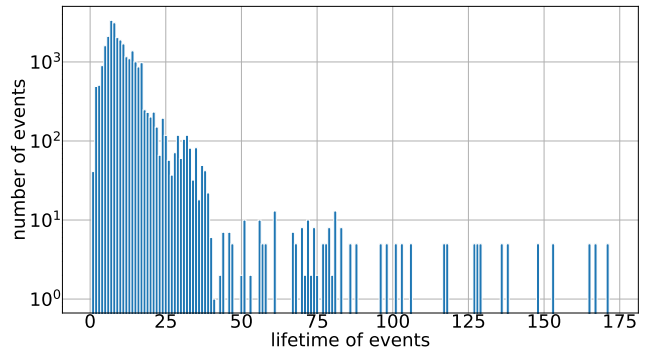


Fig. 5: The distribution of events lifetime.

D. Analysis time

The analysis time includes the time to pre-compute the matrices and the duration of the pipeline analysis on the CFG. We run the analysis on a virtual machine on a cloud server with 8 GB RAM and 4-core Intel Broadwell processors. Only 2 cores are occupied simultaneously to process the benchmarks. We also measure the analysis time without leveraging the algebraic property of XDD to pre-compute the matrices (with a timeout of 1 hour) in order to clarify the benefit of this optimization. The results are shown in Figure 6. The x-axis shows the benchmarks and the y-axis plots the analysis time in seconds in a logarithmic scale. The analysis time with matrices is shown as green bars. At worst, the analysis with matrices finishes in 553s (9m13s). In most cases, it finishes in about 1 to 20s. In contrast, the analysis without matrices has both memory usage and speed issues as shown

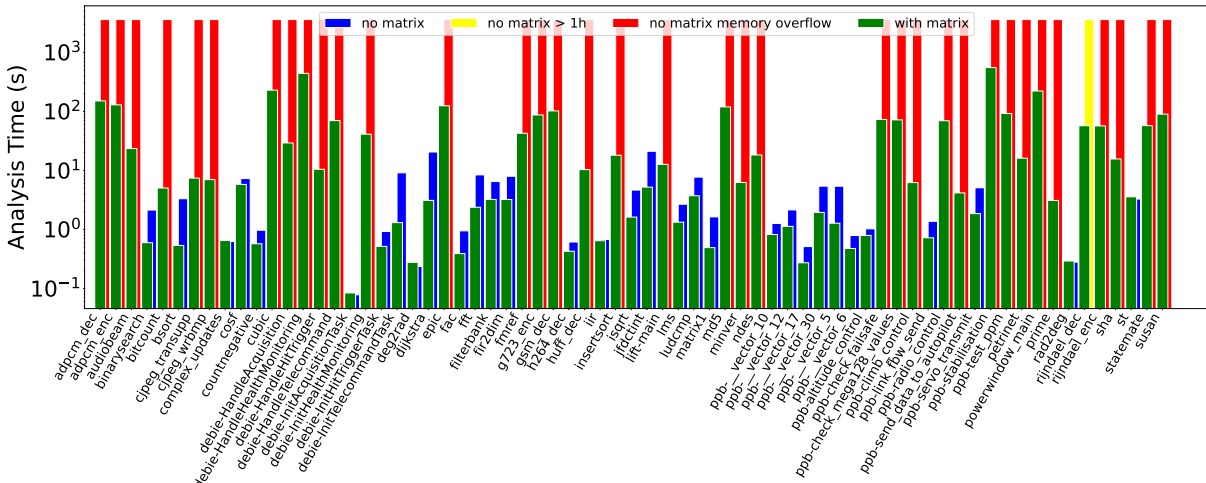


Fig. 6: The analysis time.

by the red (crashed because out of 8G RAM) and yellow bars (timeout after 1 hour). For those finishing within 1 hour (blue bars), the matrix optimization brings 217% speed-up in average⁶. The rare cases where the analysis without matrix is faster are simple benchmarks where the cost of computing the matrices is not balanced by the speed-up. This result reveals that the pre-computation of matrices effectively reduces intermediate redundant computations, which enhances the analysis performance in terms of speed and memory usage. The analysis is still able to handle problematic cases (those that have a large number of temporal states or long lifetime events) in a reasonable time. Moreover, we observe that the industry-like applications encompassed in the TACLeBench collection (Debbie and Papabench) are analyzed in short times (respectively 10 and 15 minutes, summing the analysis times of all their tasks). Therefore, we believe that our approach could be used in industrial real-time applications (for example, Airbus requires at most 48 hours between the detection of a bug and the distribution of the fix, including temporal verification).

E. Precision

The presence of out-of-order resources enables potential timing anomalies [7]. This means that the pipeline analysis can not assume the local worst case to be the global worst case upon timing variations. In the presence of possible timing anomalies, a trade-off between precision and performance is more difficult to achieve: the analysis either has to track exactly all possible timing states or to cover the timing variations with a safe but largely over-estimated cost. In the example of the shared bus, the cost for not tracking precise pipeline states is to cover the latency of memory access with an upper bound by considering the maximal potential contention with prior and subsequent instructions. To evaluate this over-estimation, we implemented this strategy in *etime*, the state-of-the-art pipeline

⁶average speed up = the sum of the analysis times of all the benchmarks without matrix divided by the sum of analysis times with matrices.

analysis of OTAWA. We compare the WCET estimated with *etime* to the one estimated with the new approach.

Concretely, the *etime* analysis implements the same pipeline model (i.e. XG based) except for it does not use XDDs and considers the WCET of BBs locally instead of at CFG-level. In order to tighten the WCET, it considers all the combinations of events for each BB. But since it disregards the execution context, it may choose to drop the context at any time to reduce the exponential number of pipeline states – which is not safe with timing anomalies. Moreover, *etime* generates only one execution time for each BB (the worst one), while the new pipeline analysis provides all the possible execution times to the IPET stage. The way IPET can handle these multiple execution times has been detailed in [31] and is out of the scope of this paper, but it clearly benefits the new approach. Finally, as *etime* originally did not support out-of-order accesses, we created a new type of event with a latency of one memory access that is associated to each memory access not classified as Always Hit or Always Miss in order to cover the waiting time of the shared bus.

As both *etime* and the approach presented in this paper are implemented with *OTAWA*, we are able to ensure that the micro-architectural model and global analyses are the same. Disregarding the safety issue due to ignoring timing anomalies, we believe that the WCET obtained by *etime* can be used as a reference of a classical static WCET approach that considers out-of-order resources without tracking exact pipeline states.

The experimental results are shown in Figure 7, in which the x-axis shows the benchmarks and the y-axis shows the gain in precision computed by $(t_{etime} - t_{new})/t_{etime}$, where t_{etime} is the WCET obtained by *etime* and t_{new} is the WCET obtained by our new approach. Due to the limited performance of *etime*, the *epic* benchmark does not finish within 6 hours. The *susan* benchmark also fails due to a bug in *OTAWA*. This is why the bars for these two benchmarks miss in the figure.

The experimental results show that, for most of the benchmarks, the WCET obtained by using the new approach is improved by 40% to 80%. In some rare cases (*fft*, *two*

- [3] T. Lundqvist and P. Stenstrom, "Timing anomalies in dynamically scheduled microprocessors," in *IEEE RTSS*, 1999.
- [4] J. Eisinger, I. Polian, B. Becker, S. Thesing, R. Wilhelm, and A. Metzner, "Automatic Identification of Timing Anomalies for Cycle-Accurate Worst-Case Execution Time Analysis," in *IEEE DDECS*, 2006.
- [5] G. Gebhard, "Timing anomalies reloaded," in *WCET 2010*.
- [6] F. Cassez, R. R. Hansen, and M. C. Olesen, "What is a timing anomaly?" in *WCET*, 2012.
- [7] I. Wenzel, R. Kirner, P. Puschner, and B. Rieder, "Principles of timing anomalies in superscalar processors," in *QSIC'05*.
- [8] R. Wilhelm, S. Altmeyer, C. Burguière, D. Grund, J. Herter, J. Reineke, B. Wachter, and S. Wilhelm, "Static Timing Analysis for Hard Real-Time Systems," in *VMCAI*, 2010.
- [9] Y.-T. S. Li and S. Malik, "Performance analysis of embedded software using implicit path enumeration," in *ACM SIGPLAN LCTES*, 1995.
- [10] H. Falk, S. Altmeyer, P. Hellinckx, B. Lisper, W. Puffitsch, C. Rochange, M. Schoeberl, R. B. Sørensen, P. Wagemann, and S. Wegener, "Taclebench: A benchmark collection to support worst-case execution time research," in *WCET*, 2016.
- [11] C. Ballabriga, H. Cassé, C. Rochange, and P. Sainrat, "Ottawa: An open toolbox for adaptive wcet analysis," in *IFIP SEUS*, 2010.
- [12] J. Schneider and C. Ferdinand, "Pipeline behavior prediction for superscalar processors by abstract interpretation," *ACM SIGPLAN Notices*, vol. 34, no. 7, pp. 35–44, May 1999.
- [13] S. Thesing, "Safe and precise wcet determination by abstract interpretation of pipeline models," Ph.D. dissertation, Univ. Saarland, 2004.
- [14] P. Cousot and R. Cousot, "Abstract interpretation: a unified lattice model for static analysis of programs by construction or approximation of fixpoints," in *4th ACM SIGACT-SIGPLAN symposium on PLDI*, 1977.
- [15] S. Wilhelm, "Symbolic representations in WCET analysis," Ph.D. dissertation, Saarland University, 2012.
- [16] J. Reineke and R. Sen, "Sound and Efficient WCET Analysis in the Presence of Timing Anomalies," in *WCET'09*, 2009.
- [17] S. Hahn, J. Reineke, and R. Wilhelm, "Toward Compact Abstractions for Processor Pipelines," ser. LNCS, 2015, vol. 9360, pp. 205–220.
- [18] S. Hahn and J. Reineke, "Design and analysis of SIC: a provably timing-predictable pipelined processor core," *Real-Time Systems*, vol. 56, 2020.
- [19] J. Engblom and B. Jonsson, "Processor pipelines and their properties for static WCET analysis," 2002.
- [20] X. Li, A. Roychoudhury, and T. Mitra, "Modeling out-of-order processors for software timing analysis," in *IEEE RTSS*, 2004.
- [21] C. Rochange and P. Sainrat, "A Context-Parameterized Model for Static Analysis of Execution Times," in *HIPEAC II*, ser. LNCS, 2009.
- [22] G. Behrmann, A. David, K. G. Larsen, J. Håkansson, P. Pettersson, W. Yi, and M. Hendriks, "Uppaal 4.0," 2006.
- [23] F. Cassez, "Timed games for computing wcet for pipelined processors with caches," in *IEEE ACSD*, 2011.
- [24] S.-S. Lim, Y. H. Bae, G. T. Jang, B.-D. Rhee, S. L. Min, C. Y. Park, H. Shin, K. Park, S.-M. Moon, and C. S. Kim, "An accurate worst case timing analysis for risc processors," *IEEE transactions on software engineering*, vol. 21, no. 7, pp. 593–604, 1995.
- [25] A. Colin and I. Puaut, "A modular and retargetable framework for tree-based wcet analysis," in *Proceedings 13th Euromicro Conference on Real-Time Systems*. IEEE, 2001, pp. 37–44.
- [26] R. Kirner, A. Kadlec, and P. Puschner, "Precise worst-case execution time analysis for processors with timing anomalies," in *2009 21st Euromicro Conference on Real-Time Systems*, 2009, pp. 119–128.
- [27] J. Engblom and B. Jonsson, "Processor pipelines and their properties for static wcet analysis," in *International Workshop on Embedded Software*. Springer, 2002, pp. 334–348.
- [28] S. B. Akers, "Binary decision diagrams," *IEEE Transactions on computers*, vol. 27, no. 06, pp. 509–516, 1978.
- [29] R. E. Bryant, "Symbolic boolean manipulation with ordered binary-decision diagrams," *ACM Computing Surveys (CSUR)*, 1992.
- [30] M. Fujita, P. C. McGeer, and J.-Y. Yang, "Multi-terminal binary decision diagrams: An efficient data structure for matrix representation," *Formal methods in system design*, vol. 10, no. 2, pp. 149–169, 1997.
- [31] Z. Bai, H. Cassé, M. De Michiel, T. Carle, and C. Rochange, "A framework for calculating wcet based on execution decision diagrams," *ACM TECS*, 2022.